Functional Reconstitution of Rhodopsin into Tubular Lipid Bilayers Supported by Nanoporous Media†

Olivier Soubias, Ivan V. Polozov, Walter E. Teague, Alexei A. Yeliseev, and Klaus Gawrisch*

Laboratory of Membrane Biochemistry and Biophysics, NIAAA, National Institutes of Health, Bethesda, Maryland 20892

Received July 14, 2006; Revised Manuscript Received October 20, 2006

ABSTRACT: We report on a novel reconstitution method for G-protein-coupled receptors (GPCRs) that yields detergent-free, single, tubular membranes in porous anodic aluminum oxide (AAO) filters at concentrations sufficient for structural studies by solid-state NMR. The tubular membranes line the inner surface of pores that traverse the filters, permitting easy removal of detergents during sample preparation as well as delivery of ligands for functional studies. Reconstitution of bovine rhodopsin into AAO filters did not interfere with rhodopsin function. Photoactivation of rhodopsin in AAO pores, monitored by UV−vis spectrophotometry, was indistinguishable from rhodopsin in unsupported unilamellar liposomes. The rhodopsin in AAO pores is G-protein binding competent as shown by a [^{35}S]GTPγS binding assay. The lipid−rhodopsin interaction was investigated by ^{2}H NMR on *sn*-1- or *sn*-2-chain perdeuterated 1-stearoyl-2-docosahexaenoyl-*sn*-glycero-3-phospholine as a matrix lipid. Rhodopsin incorporation increased mosaic spread of bilayer orientations and contributed to spectral density of motions with correlation times in the range of nano- to microseconds, detected as a significant reduction in spin−spin relaxation times. The change in lipid chain order parameters due to interaction with rhodopsin was insignificant.

Structural and functional studies on purified membrane proteins are very challenging because of difficulties with sample preparation. The most widely used protocols consist of detergent solubilization of proteins, addition of lipid to the micellar solution, formation of membrane vesicles by detergent removal or by rapid dilution below the critical micelle concentration (cmc) followed by detergent removal with polystyrene beads via hydrophobic adsorption (*1*−*3*), dialysis (*4*, *5*), column chromatography (*6*−*8*), or a combination of the three approaches (*9*, *10*). The commonly used procedures for detergent removal are time-consuming, may result in a substantial loss of precious material, and could be detrimental for protein activity. Here, it was explored whether the reconstitution of rhodopsin into a porous anodic aluminum oxide (AAO) substrate is a better way to quickly form GPCR-containing bilayers that are free of detergent.

The following goals were set: the reconstituted protein must be functional, reconstitution should be completed within minutes, one side of the membrane must be freely accessible from the water phase, bilayers should be oriented, and membrane concentration should be sufficiently high to enable structural studies by NMR and diffraction methods. A promising approach is to deposit membranes inside the pores of AAO filters as single, tubular bilayers. Anodic oxidation of aluminum produces γ-alumina with a reproducible pore size in the submicrometer range, high pore density, and a narrow pore size distribution. Several laboratories reported feasibility of depositing phospholipid layers on the cylindrical walls of AAO pores (*11*−*14*). The tubular lipid bilayers cover pore walls over their entire length. A porous AAO filter with a surface area of 1 cm^2 and a thickness of 60 μm allows a very high density of solid-supported single bilayers per filter, which for a typical phospholipid can be as high as ∼250 to 300 μg of lipids per filter.

We previously reported on the formation of tubular lipid bilayers by extrusion of multilamellar liposomes through AAO filters and characterized their properties by ^{1}H-, ^{2}H-, and ^{31}P solid-state NMR with and without magic angle spinning (MAS) (*15*). In the fluid bilayer phase, membranes were unperturbed by the solid support. Mosaic spread of bilayer orientations exceeded mosaic spread of pore orientation considerably, indicating that bilayers do not adhere strictly to the solid surface, but form wavy tubules with a 3 nm (on average) wide water layer between the membranes and the AAO surface. We successfully trapped the water-soluble polymer PEG 8000 in this water layer. Diffusion experiments by NMR demonstrated that bilayer tubules consisted of short pieces with an average length of less than 1 μm. They adhere to the AAO surface at their ends, such that the water layer trapped between AAO and bilayers is sealed off from the water column in the middle of the pores. However, the seal can be broken by forceful flushing or by decreasing the temperature below the gel phase transition of lipids.

Porous AAO has been used to study the interaction of protein with membranes (*16*). We used AAO filters for reconstitution of rhodopsin to conduct ^{1}H MAS NMR experiments with magnetization transfer from protein to lipids (*17*) as well as for reconstitution of recombinant human cannabinoid receptor CB2 (*18*). Other laboratories reported the first spectra of labeled peptides reconstituted into tubular bilayers in porous AAO (*19*−*21*).

† This work was supported by the Intramural Research Program of NIAAA, NIH.

* Corresponding author. Phone: (301)594-3750. Fax: (301)594-0035. E-mail: gawrisch@helix.nih.gov.

10.1021/bi061416d
Published on Web 12/09/2006

Here, we demonstrate that the GPCR rhodopsin retains function upon reconstitution into porous AAO filters. Rhodopsin represents a paradigm for the large and diverse family of GPCR that plays an essential role in the transduction of signals from the extracellular environment across the plasma membrane to the interior of eukaryotic cells and thus are important pharmacological targets. Rhodopsin was reconstituted into a lipid matrix with polyunsaturated, docosahexaenoic acid (DHA, 22:6n3) hydrocarbon chains to simulate its natural environment. Reconstitution at concentrations sufficient for NMR structural studies was achieved within minutes. Structural transitions of rhodopsin after photoisomerization of retinal were unperturbed by the solid support. The activated receptor was G-protein binding competent. Perturbations of lipid chain order due to the presence of the protein are very small. However, rhodopsin increased mosaic spread of bilayer orientations and significantly reduced ^{2}H spin−spin relaxation times.

MATERIALS AND METHODS

Lipids. The phospholipids 1-perdeutero-stearoyl-2-docosahexaenoyl-*sn*-glycero-3-phosphocholine (18:0d35-22:6n3-PC), 1-stearoyl-2-perdeutero-docosahexaenoyl-*sn*-glycero-3-phosphocholine (18:0-22:6d31n3-PC), and 1-palmitoyl-2-oleolyl-*sn*-glycero-3-phosphocholine (16:0-18:1n9-PC) were synthesized by Avanti Polar Lipids Inc. (Alabaster, AL). Perdeuterated DHA was produced by growing *Crypthecodinium cohnii* (Martek Biosciences, Inc.) on 50% deuterated water. According to high resolution ^{1}H and ^{2}H NMR experiments, the DHA chain was deuterated to 38%, except for the terminal methyl group, which was deuterated to 30%. Polyunsaturated lipids were stored at −80 °C in sealed, argon-filled ampules as a solution in methylene chloride with the antioxidant butylated hydroxytoluene (BHT) added at a lipid/BHT molar ratio of 200:1. Texas Red−DHPE for fluorescence labeling of the lipid matrix was obtained from Invitrogen (Carlsbad, CA).

Bovine Rhodopsin. Rhodopsin was purified from bovine retinas using previously published procedures (*22*). Rhodopsin fractions that gave a 280/500 nm intensity ratio of 1.9 or lower in the UV−vis absorption spectra were used for reconstitution. Particular care was taken to remove traces of retinal lipids including cholesterol from the preparation. Residual lipid content was monitored by choline and cholesterol assays. Only rhodopsin fractions with less than 0.3 molecules of cholesterol per rhodopsin were selected.

Reconstitution into AAO Pores. To reconstitute rhodopsin into lipid bilayers, a micellar solution of rhodopsin and lipid in octylglucoside (OG) was rapidly diluted below the cmc of OG (19 mM) by injection into PIPES buffer (10 mM Pipes, 100 mM NaCl, 50 μM DTPA, pH 7.0) prepared with deuterium-depleted water. The final concentration of OG after dilution was 10 mM or less. Tubular rhodopsin-containing bilayers were formed by extrusion of proteoliposomes through Anopore filters (Whatman) with a nominal pore diameter of 0.2 μm and a thickness of 60 μm. Extrusion was performed in a stainless steel thermobarrel extruder (Lipex Biomembranes, Inc., Vancouver, BC, Canada) at ambient temperature, well above the main phase transition temperature of 16:0-18:1n9-PC (271 K) and 18:0-22:6n3-PC (271 K). For each experiment, from two to five AAO filters (Ø 13 mm) were stacked and flushed with several millileters of PIPES buffer before extruding the dispersion of proteoliposomes. 1 mL of proteoliposome dispersion (0.3−0.7 mg lipids/mL) was then extruded five times through the stack of filters at a rate of 0.01 mL/s resulting in entrapment of multilamellar structures inside the pores. All but a single bilayer near the AAO pore surface, as well as residual OG in membranes, were removed by flushing the filters with 5 mL of PIPES buffer at a rate of 0.2 mL/s. The lipid concentration in the proteoliposome dispersion before and after extrusion was measured by following the fluorescence intensity of 0.1% Texas Red−DHPE that was added to the lipid. The rhodopsin concentration was determined by light absorption at 498 nm. Samples were prepared in complete darkness in a glove box filled with pure nitrogen gas, generated from liquid nitrogen, to prevent oxidation of the polyunsaturated lipid.

^{2}H NMR. Solid-state ^{2}H NMR experiments were carried out on a Bruker DMX500 spectrometer equipped with a flat coil probe (Doty Scientific, Columbia, SC). Data were acquired at a temperature of 308 K with a quadrupolar echo pulse sequence (*23*) of $d_1-90°_x-\tau-90°_y-$acq, a relaxation delay time of $d_1 = 250$ ms, a 5 μs 90° pulse, a delay time of $\tau = 75$ μs, and a 200 kHz spectral width. Typically, 200 000 transients were acquired. ^{2}H NMR spin−spin relaxation times (T_2) were measured with a quadrupolar spin echo experiment ($\pi/2-\tau-\pi/2-$acq) following the reduction of signal intensity with increasing delay time, τ. To improve spectral resolution, the experiments on the randomly deuterated *sn*-2 chain were performed with proton decoupling. The spin−spin relaxation times, T_{1q}, were measured by an inversion−recovery pulse sequence ($\pi-\tau-\pi/2-$acq).

Photoactivation of Rhodopsin. UV−vis absorption spectra of rhodopsin were recorded at 291 K with a Hewlett-Packard 8452A diode array spectrophotometer. Measurements were conducted on a single AAO filter containing ∼120−160 μg of rhodopsin reconstituted into 16:0-18:1n9-PC or 18:0-22:6n3-PC bilayers at a protein/lipid molar ratio of 1:100. The water in AAO pores was replaced by a 5 M sucrose solution to match refractive indices of pores and AAO substrate. This reduced the scattering of light from AAO filters to acceptable levels. The filters were mounted on the inner surface of a cuvette with a path length of 1 cm, filled with a 5 M sucrose solution. Four consecutive UV−vis absorption spectra were recorded over the wavelength range 300−800 nm. Spectrum 1 was from unbleached rhodopsin. Light exposure from the instrument was sufficiently low to prevent a measurable bleaching of rhodopsin, as confirmed by repeating the experiment. Spectrum 2 was taken immediately after exposure to a single flash from a Metz 451 camera strobe passed through a 500 nm interference filter (bandwidth 25 nm). Spectrum 3 was acquired after addition of 30 μL of a freshly prepared 2 M hydroxylamine solution in PIPES buffer at pH 7 to the sucrose solution. Spectrum 4 was obtained after exposure to the light of a green laser pointer (wavelength 532 nm, power 5 mW) for 60 s (Figure 4).

Although scattering was reduced by the high sucrose concentration in solution, it was necessary to correct the spectral baseline for the influence of light scattering. This was done by fitting spectral baselines over the spectral ranges 350−450 nm and 600−800 nm (spectra 1−3, Figure 4) and 450−800 nm (spectrum 4, Figure 4) to a polynomial function

of fourth-order and subtracting the fitted baseline from the spectrum over the entire recorded range. The difference spectrum (*2*−*3*), with an absorption maximum at 478 nm, corresponds to the spectrum of metarhodopsin-I (MI). Therefore, an additional criterion for acceptance of the baseline correction was that the baseline-corrected spectrum had the proper absorption maximum.

Gα$_{i1}$ Binding to Rhodopsin. Gα$_{i1}$ was expressed in *Escherichia coli* and purified as described earlier (*24*). The 30 μL of proteoliposome dispersion in PIPES buffer, containing 1 nmol/mL of rhodopsin at a rhodopsin/16:0-18:1n9-PC molar ratio of 1:1000, was extruded by centrifugation (6 min, 2000*g*) through one AAO filter (tissue culture inserts with a 0.2 μm Anopore ,membrane, Nalge Nunc International, Rochester, NY). The amount of lipid in AAO filters was measured by recording the fluorescence of 0.1% Texas Red−DHPE in the bilayers before and after filtration. The filters were washed twice with PIPES buffer (30 μL, 1 min, 10000*g*) to remove all but the last tubular membrane layer at the pore surface. Rhodopsin was bleached by exposing samples to the light of a green laser pointer for 60 s. Within 1 min, rhodopsin was exposed to a solution of Gα$_{i1}$ (30 μL, 5.33 nmol/mL Gα$_{i1}$, 50 mM MOPS buffer, pH 7.5, 100 mM NaCl, 11 mM $MgSO_4$, 1 mM EDTA, 1 mM DTT) that was sent through the filter by centrifugation (6 min, 2000*g*). The filters were then washed twice with MOPS buffer (30 μL, 1 min, 10000*g*) to remove excess Gα$_{i1}$ that did not bind to rhodopsin. GDP−GTPγS exchange was performed by exposing filters to 30 μL of a 41 μM solution of [^{35}S]GTPγS/GTPγS, molar ratio 0.0043, in MOPS buffer as above that was sent through the filter by centrifugation at 2000*g*. The filters were then washed twice with MOPS buffer (30 μL, 1 min, 10000*g*) to collect Gα$_{i1}$−GTPγS complexes, and the eluted volume was mixed with 1 mL of chilled stop buffer (20 mM Tris−HCl, pH 8.0, 100 mM NaCl, 25 mM $MgCl_2$, 4 °C). The eluent was filtered immediately through a nitrocellulose membrane that trapped the Gα$_{i1}$−GTPγS complex (retention efficiency 80% (*25*)). The nitrocellulose filter was washed three times with 1 mL of stop buffer and air-dried. The amount of filter-bound [^{35}S]GTPγS was determined by scintillation counting using 4 mL of scintillation cocktail Scintisafe Plus 50% from Fisher Scientific (Pittsburgh, PA). In order to quantify the rhodopsin-containing membranes on the AAO filters, they were eluted from filters with a 1% SDS solution. The quantity of eluted lipid was measured via the fluorescence intensity of the Texas Red−DHPE marker.

RESULTS

Quantitative Loading. Proteoliposomes were prepared and extruded through two stacked AAO filters. The amount of lipid and rhodopsin in the AAO filter pores, reproducibility of loading, and the protein/lipid ratio were monitored by UV−vis spectrophotometry on rhodopsin and the Texas Red−DHPE fluorescence intensity. A buildup of multiple bilayers at the AAO pore walls was removed by flushing pores with buffer. The amount of rhodopsin and lipids retained inside the pores was measured by recording concentrations of rhodopsin and lipids before and after extrusion, as well as in the wash fractions. Experiments were conducted at two protein/lipid molar ratios, 1:1000 and 1:100. Protein/lipid ratios before and after extrusion were identical, indicating that neither protein nor lipid were selectively retained by AAO. At a protein/lipid ratio of 1:100, one AAO filter (exposed filter area 1.32 cm^2) retained 90 μg of rhodopsin and 200 μg of lipid. Assuming a pore density of 1.6×10^9 pores/cm^2 (calculated from filter porosity reported by Whatman), a pore diameter of 0.2 μm, and a filter thickness of 60 μm, the total exposed pore wall area is ∼600 cm^2. The 200 μg of lipids corresponds to a bilayer area of 470 cm^2, and the 90 μg of rhodopsin corresponds to an area of 125 cm^2, assuming a rhodopsin lateral area of 900 Å^2 (*26*). Adding those areas yields a total membrane area of 595 cm^2, which is in good agreement with the estimated area of pore walls. Reproducibility of filter loading with single, tubular bilayers was within a few percent.

Tubular Geometry—Lipid Order. The properties of bilayers at the pore walls were characterized by ^{2}H NMR on 18:0d35-22:6n3-PC with *sn*-1 chain perdeuterated stearic acid. AAO filters were oriented with their filter normal parallel to the B_0 magnetic field of the NMR instrument (pore axes parallel to the magnetic field). Order parameter profiles, mosaic spread of bilayer orientations, and resonance line width were determined by fitting the spectra with a program written for Mathcad (Mathsoft) (*15*). The program reported a smoothed order parameter profile of lipid hydrocarbon chains, the orientational distribution function of bilayer normals (assumed to be Gaussian), and the resonance line width of all resolved quadrupolar splittings. The experimental and simulated spectra as a function of protein/lipid ratio are shown in Figure 1A.

The order parameter profile of the saturated stearic acid chains in AAO filters was compared with order in fully hydrated, multilamellar liposomes. With increasing protein content, both mosaic spread of bilayer orientations and homogeneous line broadening increased. The latter correlated with shorter spin−spin relaxation times, T_2.

The orientational distribution function of bilayer normals indicated unambiguously that bilayers have cylindrical symmetry. The cylinder axes are oriented parallel to the AAO filter normal, in agreement with bilayers lining the walls of the 0.2 μm wide and 60 μm long pores that traverse AAO filters. The order parameter profile of 18:0-22:6n3-PC in tubular lipid bilayers was indistinguishable from order in fully hydrated, multilamellar liposomes. Because an OG content in bilayers of less than 3 mol % is sufficient to induce measurable order changes, this also confirms that OG was very effectively removed from the tubular bilayers by flushing filters with buffer. Experiments on plain 18:0-22:6n3-PC bilayers yielded a width of the Gaussian distribution of bilayer orientations of 8° and a homogeneous line broadening of 500 Hz, corresponding to a $T_2 = 0.64$ ms.

The experiment was repeated at increasing concentrations of dark-adapted rhodopsin in the range 1000−100 lipids per rhodopsin. Lipid order parameter profiles were almost independent of protein content (Figure 1A(a−e)). Even at the highest protein concentration, only a small decrease of order parameters was observed, less than 0.005 for the plateau region (hydrocarbon chain segments C2−C8, Figure 1B); no change of order for segments located in the bilayer center (C9−C18) was observed. Results were similar over the temperature range 5−40 °C. Bleaching of rhodopsin did not change order parameters. However, the presence of protein increased mosaic spread of bilayer orientations from

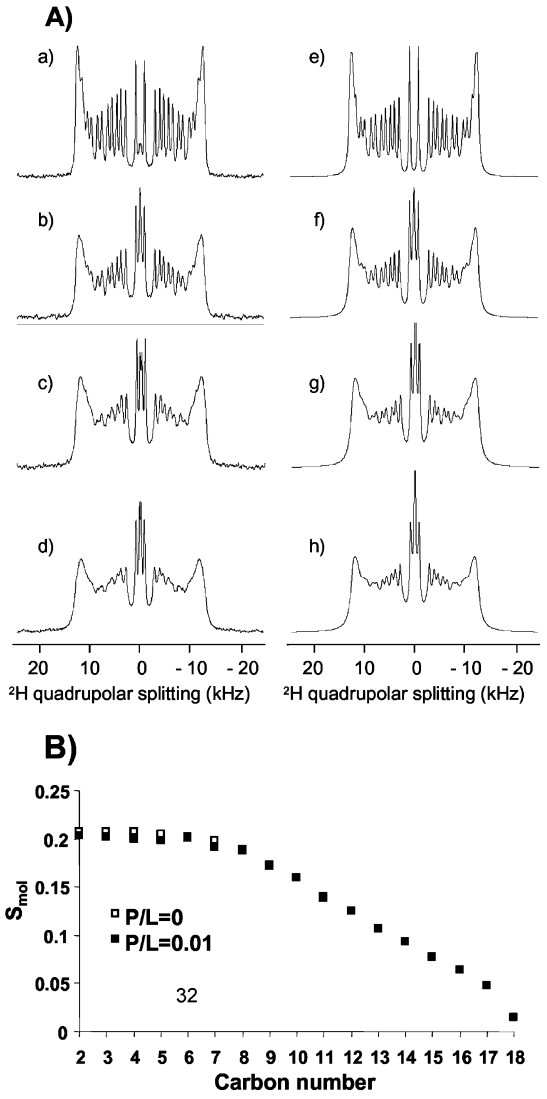

FIGURE 1: (A) (a−d) (left) Experimental ^{2}H NMR spectra of *sn*-1 chain perdeuterated 18:0d35-22:6 PC-rhodopsin tubular bilayers reconstituted into AAO filters at a rhodopsin/lipid molar ratio of 0 (a), 0.001 (b), 0.005 (c), and 0.01 (d). Samples were oriented in the magnetic field such that the axis of pores was oriented parallel to B_0. The quadrupolar splittings correspond to an orientation of bilayer normals perpendicular to the field confirming the tubular geometry of lipid bilayers inside the pores. (A) (e−h) Simulated ^{2}H spectra were obtained as reported in ref 15. The analysis yielded hydrocarbon chain order parameters (Figure 1B), the distribution of bilayer normals, including the mosaic spread, and the line width of the superimposed quadrupolar splittings (see text). (B) Order parameter profile of the *sn*-1 chain perdeuterated 18:0-22:6n3-PC at a rhodopsin/lipid molar ratio of 0 (open square) and 0.01 (filled square).

8° for bilayers without rhodopsin to 13°, 18°, and 20° at protein/lipid molar ratios of 0.001, 0.005, and 0.01, respectively. Obviously, with increasing protein content, bilayers are less likely to orient parallel to the pore walls.

A model of tubular membranes containing rhodopsin is presented in Figure 2.

Lipid Dynamics—^{2}H NMR Relaxation. Lipid dynamics were explored by measurement of lipid ^{2}H NMR spin−spin, T_2, and spin−lattice, T_{1q}, relaxation times as a function of concentration of dark-adapted rhodopsin. At all protein/lipid ratios, the dependence of signal height on relaxation delay time could be fitted by a single-exponential decay, indicating that membranes contained one homogeneous population of

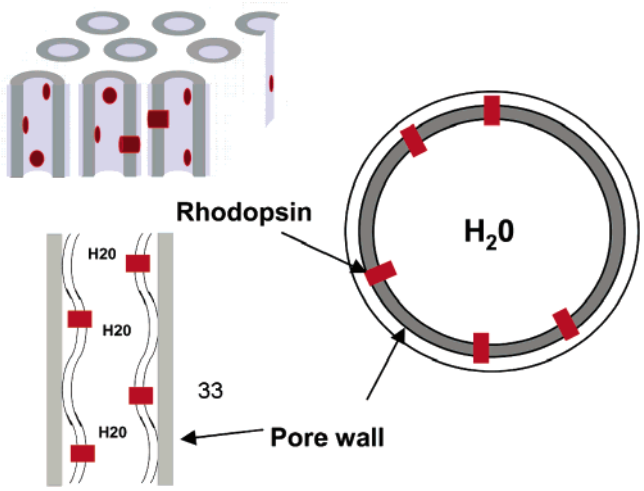

FIGURE 2: Cartoon of single tubular bilayers containing rhodopsin inside the pores of AAO filters.

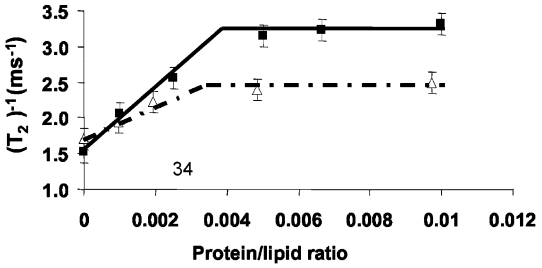

FIGURE 3: Variation of the deuterium T_2 relaxation times of both *sn*-1 chain perdeuterated 18:0d35-22:6 PC (filled squares) and *sn*-2 chain perdeuterated 18:0-22:6d31 PC (open triangles), reported as function of protein/lipid ratio. The *sn*-1 chain data represent T_2 relaxation times of methylene segments from the plateau region of order parameters, carbons C_2−C_8; *sn*-2 chain T_2 was measured for carbons C_2 and C_3.

lipids. Samples also had only one set of quadrupolar splittings, suggesting that lipids exchange rapidly between the rhodopsin interface and the bulk of the lipid matrix on a time scale of 10^{-4} s. Figure 3 shows the dependence of T_2 on rhodopsin content for both *sn*-1 perdeuterated 18:0d35-22:6n3-PC (resonances of C_{2-8}−^{2}H bonds) and of *sn*-2 chain perdeuterated 18:0-22:6n3d31-PC (resonances of $C_{2,3}$−^{2}H bonds). The presence of rhodopsin significantly reduced acyl chain T_2 relaxation times. Values for the *sn*-1 chain decreased in a linear fashion from $T_2 = 0.65$ ms of protein-free membranes to $T_2 = 0.32$ ms at a rhodopsin concentration of 250−300 lipids per rhodopsin (protein/lipid molar ratio ~0.004) and remained constant down to 100 lipids per rhodopsin (molar ratio 0.01). Results for *sn*-2 chain deuterated 18:0-22:6n3d31-PC are similar, with $T_2 = 0.57$ ms for plain lipid membranes and $T_2 = 0.43$ ms at lipid/protein ratios of 0.04 and lower.

Contrary to T_2 relaxation, the changes of spin−lattice relaxation times, T_{1q}, with increasing rhodopsin content were mostly too small to be measured reliably, assuming error limits in the range of 5−10%. We observed a small reduction of the T_{1q} values of the terminal methyl group of the *sn*-1 chain with increasing protein content. The changes are barely outside experimental error limits. In experiments on rhodopsin-containing bilayers that were oriented between glass plates, a reduction of T_{1q} of *sn*-2 chain vinyl resonances with increasing protein content was detected as well (I.V. Polozov and K. Gawrisch, unpublished work).

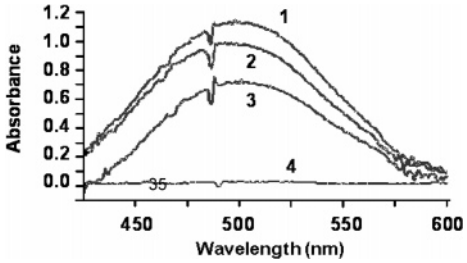

FIGURE 4: Example of a set of four successive UV−vis absorbance spectra acquired for determination of the MI/MII equilibrium of rhodopsin after partial bleaching. Rhodopsin was reconstituted into single bilayers of 18:0-C22:6n3-PC supported by porous AAO. (1) Before bleaching. (2) After partial bleaching. (3) After addition of hydroxylamine to the partially bleached sample. (4) After complete bleaching in the presence of hydroxylamine.

Photoactivation of Rhodopsin. Illumination of rhodopsin causes isomerization of the retinal chromophore, which initiates the conversion of dark-adapted rhodopsin to a metastable equilibrium between two intermediates, Metarhodopsin I and II (MI and MII) (*27*). Only the conformer MII triggers G-protein binding and activation (*28*). The MII formation is favored by low pH, high temperature, and interaction with lipids with polyunsaturated acyl chains (*29*−*31*). To detect a possible influence from the AAO support on MII formation, we reconstituted rhodopsin into 16:0-18:1n9-PC or 18:0-22:6n3-PC bilayers, measured the amount of MII formed after partial bleaching, and compared the values with previously published data that were obtained on rhodopsin in small liposomes (see Discussion).

Figure 4 shows the UV−vis absorption spectra recorded over the wavelength range 425−600 nm. Spectra were baseline-corrected, as described in the Materials and Methods. Spectrum 1 is the dark-adapted rhodopsin ($\lambda_{max} = 498$ nm). Spectrum 2 was recorded after partial bleaching by a strobe flash. It has contributions from the remaining unbleached rhodopsin as well as MI ($\lambda_{max} = 478$ nm). The superposition of spectra reveals a hypochromic shift of the maximum in spectrum 2. Spectrum 3 was recorded after addition of hydroxylamine, which left the unbleached rhodopsin intact but converted MI and MII to opsin and free retinal oxime. The spectrum reports the fraction of unbleached rhodopsin, because opsin and free retinal oxime do not adsorb at a wavelength of 450 nm and higher. Spectrum 4 is a control, acquired after complete bleaching of rhodopsin (*31*).

The amount of bleached rhodopsin (MI + MII) was determined by subtracting spectrum 3 from spectrum 1. The UV−vis absorption spectrum of pure MI was generated by subtracting spectrum 3 (unbleached rhodopsin) from spectrum 2 (MI + unbleached rhodopsin). Spectral intensities were converted to concentrations of MI and dark-adapted rhodopsin using ϵ values of 44 000 and 40 000 M^{-1} cm^{-1}, respectively (*31*). This yielded a $K_{eq} = [MII]/[MI]$ of 0.42 ± 0.1 for 16:0-18:1n9-PC and 1.0 ± 0.2 for 18:0-22:6n3-PC (Figure 4).

Gα$_{i1}$ Binding to Rhodopsin. It was shown previously that the rhodopsin-stimulated GTPase activity of $G_{i\alpha}$ is comparable or slightly higher than that of $G_{t\alpha}$ (*32*). Northup and colleagues determined that $G_{t\alpha}$ forms a complex with MII with a dissociation constant of $K_d = 10^{-7}$ M (*25*). The rhodopsin-containing bilayers in the AAO filter pores were exposed to $G\alpha_{i1}$ for complexation with the MII photointermediate. The exchange of GDP for GTPγS results in formation of a nonhydrolyzable $G\alpha_{i1}$−GTPγS complex that is released from rhodopsin. The $G\alpha_{i1}$−GTPγS complex was eluted from AAO pores, trapped on a nitrocellulose filter, and the amount of [^{35}S]GTPγS quantified by scintillation counting (Figure 5A). Figure 5B reports radioactivity measurements averaged over eight filters after $G\alpha_{i1}$ exposure to dark-adapted rhodopsin (left) and bleached rhodopsin (right). The amount of lipid membranes per AAO filter was determined by following fluorescence intensity of 0.1 mol % Texas Red−DHPE that was added as tracer. Losses of MII due to conversion to opsin were deemed to be negligible on the time scale of the experiment. Therefore, the difference in concentrations of $G\alpha_{i1}$−GTPγS between dark-adapted and bleached rhodopsin is proportional to the amount of G-protein binding-competent MII photointermediate. The concentration of $G\alpha_{i1}$−GTPγS was on the order of 40% of the estimated MII concentration.

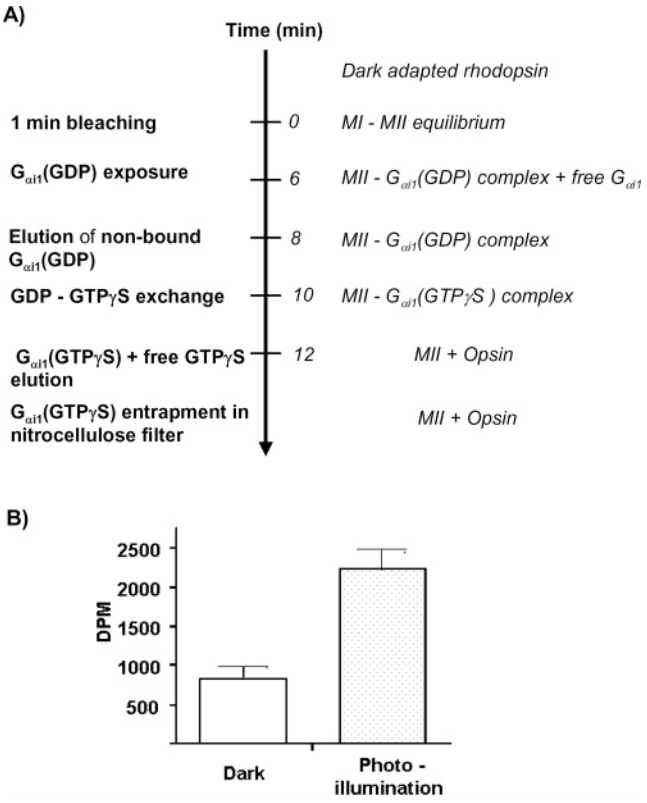

FIGURE 5: (A) Protocol of the $G\alpha_{i1}$ binding experiment. (B) Concentration of $G\alpha_{i1}$−GTPγS released from dark-adapted and bleached rhodopsin in porous AAO. The assay was performed as described in the Material and Methods. Results are averages over eight experiments.

DISCUSSION

Reconstitution of Rhodopsin. Reconstitution of rhodopsin into single, tubular lipid bilayers, supported by porous AAO substrates, yielded functional rhodopsin. Neither the lipid matrix properties nor the equilibrium of MI/MII photointermediates were different from unsupported unilamellar liposomes. The volume density of supported membranes was sufficient for solid state ^{2}H NMR studies.

Sample preparation included formation of proteoliposomes by rapid dilution of a micellar solution of phospholipids,

rhodopsin, and OG, followed by extrusion of proteoliposomes through the pores of AAO. Loading of AAO filters with tubular bilayers was rapid and highly reproducible. All but the first bilayer at the walls of AAO pores were easily washed out by flushing with buffer, as determined from estimates of the covered area of pore walls. Flushing removed residual detergent from the bilayers as well. Reproducibility of AAO loading with reconstituted bilayers was ±5 % or better. The protein/lipid molar ratio in the tubular bilayers was identical to the ratio in the solution of mixed micelles; neither rhodopsin nor the phosphatidylcholines were selectively retained by AAO. Porous AAO (1 cm^2) (thickness 60 μm, 0.2 μm nominal pore size, $\sim 10^9$ pores per cm^2) retained $\sim$200 μg of membranes containing rhodopsin at a protein/lipid molar ratio of 1:100. It is feasible to stack up to 100 filters in one experiment, yielding milligram quantities of reconstituted GPCR per sample, arranged in single, oriented lipid bilayers that are freely accessible at one side from the water phase. Sample preparation is simple and rapid, without loss of lipid or protein. The short preparation time of a few minutes per filter is beneficial for the reconstitution of labile proteins. Of particular importance is the very efficient removal of residual detergent from the bilayers, afforded by the convenience of sending buffer through pores. Rates of detergent removal are only limited by detergent flip−flop between lipid layers and the rate of detergent migration from the outer monolayer to the water phase.

Rhodopsin Photoactivation. By UV−vis spectrophotometry and G-protein binding experiments, we established that rhodopsin function was unperturbed by the solid support. In 18:0-22:6n3-PC membranes (molar ratio of protein/lipid = 0.01, 18 °C), a K_{eq} = MII/ MI = 1.0 ± 0.1 was obtained, in good agreement with the value of 1.0 ± 0.02 (same molar ratio, 20 °C) (*33*). As expected, the K_{eq} of rhodopsin in 16:0-18:1n3-PC membranes was lower (0.44 ± 0.1, 17 °C), in good agreement with literature data (*26*, *34*). Minor differences may have resulted from the use of sucrose solution to reduce light scattering, which lowers the chemical potential of water (*35*, *36*), as well as from the slightly different temperature.

The activated rhodopsin was G-protein binding competent. Differences in concentration of $G\alpha_{i1}$−GTPγS between dark-adapted and bleached rhodopsin were rather large and are easily detected. The G-protein activation experiment greatly benefited from the large accessible surface area of lipid bilayers. Conducting the experiments with tubular bilayers supported by porous AAO yields 2 to 3 orders of magnitude stronger signals compared to measurements on a single bilayer at a flat solid interface. This intensity gain is critical for NMR and many other methods. Furthermore, the tubular bilayers are stabilized and protected by pore walls, which is beneficial for reproducibility of results.

Tubular Bilayer Properties. Distortions of membrane properties due to the solid support were not observed. The tubules were reasonably well-oriented, although there was a considerable increase of mosaic spread of bilayer orientations with increasing protein content. This increase points at additional "waviness" of tubular bilayers introduced by the protein. The mosaic spread of tubular bilayer normals in this study (20° at a lipid/protein molar ratio of 0.01) is comparable to previously reported orientational spread of bilayer normals at glass surfaces for membranes at similar rhodopsin content; see, e.g., rhodopsin/DMPC membranes studied by ^{31}P NMR (*37*) and rhodopsin/POPC membranes (*38*) analyzed by a static uniaxial distribution analysis (*39*).

The presence of protein did not alter chain order parameters, except for some minor reduction of lipid order parameters of hydrocarbon chain segments near the carbonyl group. Similar observations were reported for rhodopsin in the review by Davis (*40*). Bacteriorhodopsin reconstituted into oriented di-14:0-PC bilayers showed similar behavior as well (O. Soubias, V. Réat, and A. Milon, unpublished work). Order parameters reflect tilt of chain segments as well as their conformational freedom on the time scale of the ^{2}H NMR experiment (10 μs). Because there is almost no detectable change in lipid order parameters in the presence of rhodopsin, it can be concluded that hydrocarbon chains in the bulk of the lipid matrix and at the protein−lipid interface essentially explore the same configurational space. These findings address a long-standing controversy over the influence of rhodopsin on lipid order parameters. There has been the perception that order of lipids near integral membrane proteins may be significantly lower due to interaction with the rugged surface of the protein. Because it is difficult and time-consuming to prepare reconstituted samples by conventional methods, it may be possible that changes in lipid order parameters were introduced by sample preparation procedures, e.g., low radii of liposome curvature, presence of trace amounts of detergents, trace amounts of other lipids, or trace amounts of oxidation products due to lengthy reconstitution procedures. However, it remains to be shown if observations for reconstitution of rhodopsin are also applicable to other integral membrane proteins.

The lack of substantial changes in T_{1q} in the presence of rhodopsin indicates that fast lipid motions, mostly chain isomerization with correlation times in the range of pico- to nanoseconds, are not affected, except for some minor increase of very short correlation times of motions on the time scale of picoseconds, e.g., isomerization of the methyl terminal end of saturated hydrocarbon chains and vinyl bond isomerization in polyunsaturated chains. We had shown previously (*41*, *42*) that DHA performs surprisingly rapid bond isomerization at the methylene groups that separate the cis-locked double bonds. Apparently, those correlation times may increase somewhat near rhodopsin.

Interestingly, the presence of rhodopsin promotes a large change of lipid spin−spin relaxation times, T_2. These are sensitive to motional correlation times in the range from nano- to microseconds; the spin−lattice relaxation time (T_{1q}) is exclusively sensitive to fast motions with correlation times from pico- to nanoseconds. Obviously, spectral density of slower motions increased in the presence of rhodopsin. It is important to point out that this change was not accompanied by a significant reduction of chain order parameters. Therefore, it is unlikely that the protein introduced a new type of lipid isomerization or change of molecular tilt, which, most certainly, would have reduced order parameters as well. Rather, the presence of protein may have increased the length of motional correlation times. Alternatively, the changes in T_2 could be the result of very slow motions with negligible impact on lipid order. Considering that rhodopsin increased mosaic spread of bilayer orientation, it is conceivable that the observed T_2 effects result from lateral lipid diffusion over curved bilayer regions. We estimated that local radii of

curved surfaces with a radius of curvature of 1 μm are sufficient to yield a measurable T_2 effect without a significant reduction of order parameters.

Additional information about the rhodopsin−lipid interaction may be extracted from the relaxation rates, $1/T_2$, plotted as a function of the rhodopsin/lipid molar ratio (Figure 3). Both *sn*-1 and sn-2 chains show the same dependence: relaxation rates increase up to a protein/lipid molar ratio of ∼1:275 and remain constant down to 1:100. Concentrations up to ∼275 lipids per protein result in perturbations that increase with protein content in a linear fashion, as could have been expected from the linear increase of protein−lipid interface area. However, instead of leveling off at a value close to the expected number of boundary lipids (∼22−24 (*43*, *44*)), the relaxation rates became constant at ∼275 lipids per protein and lower. Because relaxation rates are increased because of the protein−lipid interaction, it can be concluded that near 275 lipids per protein those interactions are altered. A concentration dependence of protein oligomerization is most likely responsible for this behavior. Recently, fluorescence resonance energy transfer (FRET) experiments detected multimeric association of rhodopsin molecules in azolectin liposomes (*45*) and in bilayers of well-defined lipids of different length (*46*). Spots with higher rhodopsin density in ROS disks were observed by atomic force microscopy (*47*). However, the results of this experiment are controversial (*48*−*51*). Furthermore, a recent in vivo study established that a reduction of rhodopsin density in disk membranes increased the speed of visual transduction (*52*). This effect was linked to a reduced lateral diffusion rate (*52*) and a lower propensity for MII formation (*53*). In the same study, a dramatic decrease of MII formation with increasing rhodopsin/lipid ratio at concentrations higher than 1/250 was observed. All those results combined suggest that rhodopsin oligomerization changes at rhodopsin concentrations higher than one rhodopsin molecule per 250 lipids.

In summary, adsorption of rhodopsin-containing bilayers at the pore walls of AAO did neither result in a measurable change in protein function nor did it perturb lipid bilayer properties. Sample preparation is simple and rapid. The approach is likely to be applicable to reconstitution of other membrane proteins as well. It appears to be particularly beneficial for studies that require a change of ionic strength, pH, and addition of ligands or soluble proteins during the course of the experiment. Most importantly, it enables structural studies on membrane proteins at functional conditions.

ACKNOWLEDGMENT

We thank Drake Mitchell, Burton Litman, and Kirk Hines for helpful discussions as well as for advice on preparation of bovine ROS disks and rhodopsin purification.

REFERENCES

1. Rigaud, J. L., Levy, D., Mosser, G., and Lambert, O. (1998) Detergent removal by non-polar polystyrene beads - Applications to membrane protein reconstitution and two-dimensional crystallization, *Eur. Biophys. J. Biophys. Lett. 27*, 305−319.
2. Luca, S., White, J. F., Sohal, A. K., Filippov, D. V., van Boom, J. H., Grisshammer, R., and Baldus, M. (2003) The conformation of neurotensin bound to its G protein-coupled receptor, *Proc. Natl. Acad. Sci. U.S.A. 100*, 10706−10711.
3. Devesa, F., Chams, V., Dinadayala, P., Stella, A., Ragas, A., Auboiroux, H., Stegmann, T., and Poquet, Y. (2002) Functional reconstitution of the HIV receptors CCR5 and CD4 in liposomes, *Eur. J. Biochem. 269*, 5163−5174.
4. Hong, K., and Hubbell, W. L. (1973) Lipid Requirements for Rhodopsin Regenerability, *Biochemistry 12*, 4517−4523.
5. Keller, T., Elfeber, M., Gorboulev, V., Reilander, H., and Koepsell, H. (2005) Purification and Functional Reconstitution of the Rat Organic Cation Transporter OCT1, *Biochemistry 44*, 12253−12263.
6. Allen, T. M., Romans, A. Y., Kercret, H., and Segrest, J. P. (1980) Detergent removal during membrane reconstitution, *Biochim. Biophys. Acta 601*, 328−342.
7. Kiefer, H., Krieger, J., Olszewski, J. D., vonHeijne, G., Prestwich, G. D., and Breer, H. (1996) Expression of an Olfactory Receptor in *Escherichia coli*: Purification, Reconstitution, and Ligand Binding, *Biochemistry 35*, 16077−16084.
8. Cerione, R. A., Staniszewski, C., Benovic, J. L., Lefkowitz, R. J., Caron, M. G., Gierschik, P., Somers, R., Spiegel, A. M., Codina, J., and Birnbaumer, L. (1985) Specificity of the functional interactions of the beta-adrenergic receptor and rhodopsin with guanine-nucleotide regulatory proteins reconstituted in phospholipid vesicles, *J. Biol. Chem. 260*, 1493−1500.
9. Philippot, J., Mutaftschiev, S., and Liautard, J. P. (1983) A very mild method allowing the encapsulation of very high amounts of macromolecules into very large (1000-nm) unilamellar liposomes, *Biochim. Biophys. Acta 734*, 137−143.
10. Top, D., de Antueno, R., Salsman, J., Corcoran, J., Mader, J., Hoskin, D., Touhami, A., Jericho, M. H., and Duncan, R. (2005) Liposome reconstitution of a minimal protein-mediated membrane fusion machine, *EMBO J. 24*, 2980−2988.
11. Marchal, D., Boireau, W., Laval, J. M., Moiroux, J., and Bourdillon, C. (1998) Electrochemical measurement of lateral diffusion coefficients of ubiquinones and plastoquinones of various isoprenoid chain lengths incorporated in model bilayers, *Biophys. J. 74*, 1937−1948.
12. Marchal, D., Bourdillon, C., and Dem, B. (2001) Small-Angle Neutron Scattering by Highly Oriented Hybrid Bilayer Membranes Confined in Anisotropic Porous Alumina, *Langmuir 17*, 8313−8320.
13. Marchal, D., and, B. D. (2003) Small-angle neutron scattering by porous alumina membranes made of aligned cylindrical channels, *J. Appl. Crystallogr. 36*, 713−717.
14. Wattraint, O., Warschawski, D. E., and Sarazin, C. (2005) Tethered or Adsorbed Supported Lipid Bilayers in Nanotubes Characterized by Deuterium Magic Angle Spinning NMR Spectroscopy, *Langmuir 21*, 3226−3228.
15. Gaede, H. C., Luckett, K. M., Polozov, I. V., and Gawrisch, K. (2004) Multinuclear NMR Studies of Single Lipid Bilayers Supported in Cylindrical Aluminum Oxide Nanopores, *Langmuir 20*, 7711−7719.
16. Marchal, D., Pantigny, J., Laval, J. M., Moiroux, J., and Bourdillon, C. (2001) Rate Constants in Two Dimensions of Electron Transfer between Pyruvate Oxidase, a Membrane Enzyme, and Ubiquinone (Coenzyme Q(8)), its Water-Insoluble Electron Carrier, *Biochemistry 40*, 1248−1256.
17. Soubias, O., and Gawrisch, K. (2005) Probing Specific Lipid−Protein Interaction by Saturation Transfer Difference NMR Spectroscopy, *J. Am. Chem. Soc. 127*, 13110−13111.
18. Yeliseev, A. A., Wong, K. K., Soubias, O., and Gawrisch, K. (2005) Expression of human peripheral cannabinoid receptor for structural studies, *Protein Sci. 14*, 2638−2653.
19. Chekmenev, E. Y., Hu, J., Gor'kov, P. L., Brey, W. W., Cross, T. A., Ruuge, A., and Smirnov, A. I. (2005) ^{15}N- and ^{31}P solid-state NMR study of transmembrane domain alignment of M2 protein of influenza A virus in hydrated cylindrical lipid bilayers confined to anodic aluminum oxide nanopores, *J. Magn. Reson. 173*, 322−327.
20. Lorigan, G. A., Dave, P. C., Tiburu, E. K., Damodaran, K., Abu-Baker, S., Karp, E. S., Gibbons, W. J., and Minto, R. E. (2004) Solid-State NMR Spectroscopic Studies of an Integral Membrane Protein Inserted into Aligned Phospholipid Bilayer Nanotube Arrays, *J. Am. Chem. Soc. 126*, 9504−9505.
21. Chekmenev, E. Y., Gor'kov, P. L., Cross, T. A., Alaouie, A. M., and Smirnov, A. I. (2006) Flow-through lipid nanotube arrays for structure-function studies of membrane proteins by solid-state NMR spectroscopy, *Biophys. J. 91*, 3076−3084.
22. Litman, B. J. (1982) Purification of rhodopsin by concanavalin-A affinity-chromatography, *Methods Enzymol. 81*, 150−153.

23. Davis, J. H., Jeffrey, K. R., Bloom, M., Valic, M. I., and Higgs, T. P. (1976) Quadrupolar echo deuteron magnetic resonance spectroscopy in ordered hydrocarbon chains, *Chem. Phys. Lett. 42*, 390−394.
24. Mumby, S. M., and Linder, M. E. (1994) Myristoylation of G-protein alpha subunits, *Methods Enzymol. 237*, 254−268.
25. Fawzi, A. B., Fay, D. S., Murphy, E. A., Tamir, H., Erdos, J. J., and Northup, J. K. (1991) Rhodopsin and the retinal G-protein distinguish among G-protein beta-gamma-subunit forms, *J. Biol. Chem. 266*, 12194−12200.
26. Huber, T., Botelho, A. V., Beyer, K., and Brown, M. F. (2004) Membrane model for the G-protein-coupled receptor rhodopsin: Hydrophobic interface and dynamical structure, *Biophys. J. 86*, 2078−2100.
27. Matthews, R. G., Wald, G., Brown, P. K., and Hubbard, R. (1963) Tautomeric forms of metarhodopsin, *J. Gen. Physiol. 47*, 215−240.
28. Hofmann, K. P. (1985) Effect of GTP on the rhodopsin-G-protein complex by transient formation of extra metarhodopsin II, *Biochim. Biophys. Acta 810*, 278−281.
29. Gibson, N. J., and Brown, M. F. (1990) Influence of pH on the MI-MII equilibrium of rhodopsin in recombinant membranes, *Biochem. Biophys. Res. Commun. 169*, 1028−1034.
30. Mitchell, D. C., Straume, M., and Litman, B. J. (1992) Role of *sn*-1-Saturated, *sn*-2-Polyunsaturated Phospholipids in Control of Membrane Receptor Conformational Equilibrium: Effects of Cholesterol and Acyl Chain Unsaturation on the Metarhodopsin I in Equilibrium with Metarhodopsin II Equilibrium, *Biochemistry 31*, 662−670.
31. Straume, M., Mitchell, D. C., Miller, J. L., and Litman, B. J. (1990) Interconversion of Metarhodopsins I and II: A Branched Photointermediate Decay Model, *Biochemistry 29*, 9135−42.
32. Kanaho, Y., Tsai, S. C., Adamik, R., Hewlett, E. L., Moss, J., and Vaughan, M. (1984) Rhodopsin-enhanced GTPase activity of the inhibitory GTP-binding protein of adenylate cyclase, *J. Biol. Chem. 259*, 7378−7381.
33. Niu, S. L., Mitchell, D. C., and Litman, B. J. (2001) Optimization of receptor-G protein coupling by bilayer lipid composition II: formation of metarhodopsin II-transducin complex, *J. Biol. Chem. 276*, 42807−11.
34. Mitchell, D. C., and Litman, B. J. (1994) Effect of Ethanol on Metarhodopsin II Formation is Potentiated by Phospholipid Polyunsaturation, *Biochemistry 33*, 12752−12756.
35. Parkes, J. H., Gibson, S. K., and Liebman, P. A. (1999) Temperature and pH Dependence of the Metarhodopsin I−Metarhodopsin II Equilibrium and the Binding of Metarhodopsin II to G protein in Rod Disk Membranes, *Biochemistry 38*, 6862−6878.
36. Mitchell, D. C., and Litman, B. J. (2000) Effect of ethanol and osmotic stress on receptor conformation - Reduced water activity amplifies the effect of ethanol on metarhodopsin II formation, *J. Biol. Chem. 275*, 5355−5360.
37. Gröbner, G., Choi, G., Burnett, I. J., Glaubitz, C., Verdegem, P. J. E., Lugtenburg, J., and Watts, A. (1998) Photoreceptor rhodopsin: structural and conformational study of its chromophore 11-cis retinal in oriented membranes by deuterium solid state NMR, *FEBS Lett. 422*, 201−204.
38. Salgado, G. F. J., Struts, A. V., Tanaka, K., Krane, S., Nakanishi, K., and Brown, M. F. (2006) Solid-State ^{2}H NMR Structure of Retinal in Metarhodopsin I, *J. Am. Chem. Soc. 128*, 11067−11071.
39. Nevzorov, A. A., Moltke, S., Heyn, M. P., and Brown, M. F. (1999) Solid-State NMR Line Shapes of Uniaxially Oriented Immobile Systems, *J. Am. Chem. Soc. 121*, 7636−7643.
40. Davis, J. H. (1983) The description of membrane lipid conformation, order and dynamics by 2 H-NMR, *Biochim. Biophys. Acta 737*, 117−171.
41. Eldho, N. V., Feller, S. E., Tristram-Nagle, S., Polozov, I. V., and Gawrisch, K. (2003) Polyunsaturated Docosahexaenoic vs Docosapentaenoic Acid−Differences in Lipid Matrix Properties from the Loss of One Double Bond, *J. Am. Chem. Soc. 125*, 6409−6421.
42. Feller, S. E., Gawrisch, K., and MacKerell, A. D. (2002) Polyunsaturated Fatty Acids in Lipid Bilayers: Intrinsic and Environmental Contributions to Their Unique Physical Properties, *J. Am. Chem. Soc. 124*, 318−326.
43. Dratz, E. A., Van Breemen, J. F., Kamps, K. M., Keegstra, W., and Van Bruggen, E. F. (1985) Two-dimensional crystallization of bovine rhodopsin, *Biochim. Biophys. Acta 832*, 337−342.
44. Ryba, N. J., Horvath, L. I., Watts, A., and Marsh, D. (1987) Molecular Exchange at the Lipid−Rhodopsin Interface: Spin−Label Electron Spin Resonance Studies of Rhodopsin−Dimyristoylphosphatidylcholine Recombinants, *Biochemistry 26*, 3234−3240.
45. Mansoor, S. E., Palczewski, K., and Farrens, D. L. (2006) Rhodopsin Self-Associates in Asolectin Liposomes, *Proc. Natl. Acad. Sci. U.S.A. 103*, 3060−3065.
46. Botelho, A. V., Huber, T., Sakmar, T. P., and Brown, M. F. (2006) Curvature and hydrophobic forces drive oligomerization and modulate activity of rhodopsin in membranes, *Biophys. J.*, http://dx.doi.org/10.1529/biophysj.106.082776..
47. Fotiadis, D., Liang, Y., Filipek, S., Saperstein, D. A., Engel, A., and Palczewski, K. (2003) Atomic-force microscopy: Rhodopsin dimers in native disc membranes, *Nature 421*, 127−128.
48. Jastrzebska, B., Fotiadis, D., Jang, G. F., Stenkamp, R. E., Engel, A., and Palczewski, K. (2006) Functional and structural characterization of rhodopsin oligomers, *J. Biol. Chem. 281*, 11917−11922.
49. Fotiadis, D., Jastrzebska, B., Philippsen, A., Muller, D. J., Palczewski, K., and Engel, A. (2006) Structure of the rhodopsin dimer: a working model for G-protein-coupled receptors, *Curr. Opin. Struct. Biol. 16*, 252−259.
50. Chabre, M., and le Maire, M. (2005) Monomeric G-Protein-Coupled Receptor as a Functional Unit, *Biochemistry 44*, 9395−9403.
51. Chabre, M., Cone, R., and Saibil, H. (2003) Biophysics - Is rhodopsin dimeric in native rods?, *Nature 426*, 30−31.
52. Calvert, P. D., Govardovskii, V. I., Krasnoperova, N., Anderson, R. E., Lem, J., and Makino, C. L. (2001) Membrane protein diffusion sets the speed of rod phototransduction, *Nature 411*, 90−94.
53. Niu, S. L., and Mitchell, D. C. (2005) Effect of packing density on rhodopsin stability and function in polyunsaturated membranes, *Biophys. J. 89*, 1833−1840.

BI061416D